GEOPHYSICS, VOL. 73, NO. 3 (MAY-JUNE 2008); P. B67–B75, 9 FIGS.
10.1190/1.2890287

Case History

Spontaneous potential and redox responses over a forest ring

Stewart M. Hamilton[1] and Keiko H. Hattori[2]

ABSTRACT

Forest rings are large, circular features in boreal forests that commonly exceed 500 m in diameter and are visible on aerial photographs. A detailed study of redox conditions and spontaneous potential (SP) was carried out over a forest ring that overlies an $H_2S_{(aq)}$ accumulation. Studies included drilling, monitoring well installation, and downhole SP using both polarizing and nonpolarizing electrodes. Also measured were redox potential of groundwater and soils, concentrations of sulfur species in groundwater, and headspace concentrations of redox-sensitive gases in monitoring wells. The results show positive SP anomalies in the shallow subsurface and near-horizontal, negative-inward redox gradients in the water-saturated overburden at the edges of the ring. SP anomalies are spatially correlated with redox gradients, suggesting that the two are related. The SP anomalies may be produced in response to redox gradients as redox-active ions and polar molecules spontaneously align with the negative poles toward the oxidizing end of the gradient, i.e., toward their more electronegative neighbors. This orientation of dipoles imparts a macroscopic electrical polarity to the redox gradient and results in the observed positive electrical anomaly inside the forest ring. Ongoing oxidation reactions occurring around the periphery of the forest ring maintain strong HS^- concentration gradients, which result in an outward steady-state diffusive flux of HS^-. Electromigration of redox-active ions in the redox-induced electrical field may also contribute to maintenance of the redox gradient.

INTRODUCTION

Spontaneous potential (SP) anomalies above orebodies have been reported for over 150 years, but their cause remains a subject of debate (e.g., Vagshal and Belyaev, 2001). The anomalies over buried sulfide and graphite bodies commonly show negative voltage excursions. SP anomalies have also been noted over a variety of geologic features that are not associated with metallic deposits, such as oil reservoirs (Campbell, 1960; Pirson, 1981; Tomkins, 1990; Saunders et al., 1999) and organic waste plumes in groundwater (Nyquist and Corry, 2002).

SP surveys of the type described in this article use a stationary electrode at a base station and a mobile electrode advanced in stages across the study area to measure the voltage difference between the base station and each of the mobile stations via a connecting wire. A base-station electrode is almost invariably a nonpolarizable half-cell electrode consisting of a copper (Cu) rod immersed in a saturated solution of copper sulfate ($CuSO_4$) that is in electrolytic contact with the ground via a porous (usually ceramic) membrane.

Depending on the nature of the mobile electrode, two types of SP voltage can be measured (Timm and Moller, 2001). If a bare inert metal (usually platinum) electrode is used, the voltage is a total field measurement, which is the sum of the electrical potential between the two electrodes and the redox potential of the soils in contact with the mobile electrode (V3, Figure 1). If the mobile electrode is nonpolarizable, the electrical potential between the base station and mobile electrodes is the sole contributor to voltage (V1, Figure 1).

The redox potential (i.e., the chemical component of voltage) of the soils in contact with the mobile electrodes can be obtained by subtracting the voltage obtained using the Cu-$CuSO_4$ electrode from that obtained using the metallic electrode, provided they are closely spaced and were both measured against the same base station, or by direct measurement of the voltage between the two mobile elec-

Manuscript received by the Editor 15 March 2007; revised manuscript received 13 November 2007; published online 31 March 2008.
[1]Ontario Geological Survey, Sudbury, Ontario, Canada. E-mail: stew.hamilton@ontario.ca.
[2]University of Ottawa, Department of Earth Sciences, Ottawa, Ontario, Canada. E-mail: khattori@uottawa.ca.

trodes (V2, Figure 1). The redox potential obtained by either technique is an oxidation-reduction potential (ORP) referenced against the Cu-$CuSO_4$ half-cell and, as such, is directly related to the ORP measured against the standard hydrogen electrode (Eh) of the soil or groundwater in contact with the mobile electrodes (Hamilton et al., 2004c).

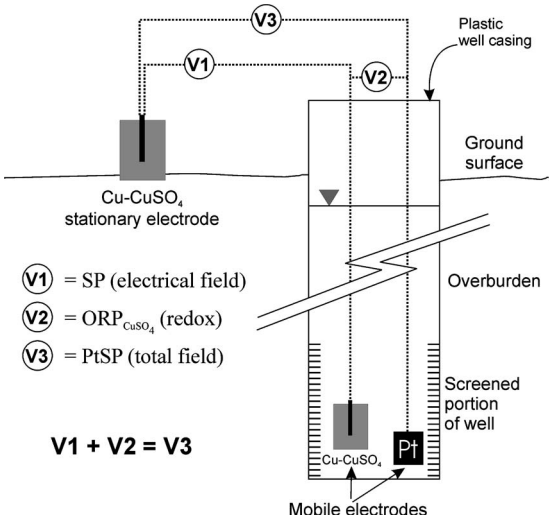

Figure 1. Diagram showing the downhole measurement technique for and relationship between electrical field (SP), total field (PtSP), and oxidation-reduction potential (ORP), referenced against the Cu-$CuSO_4$ half-cell (from Hamilton et al., 2004b).

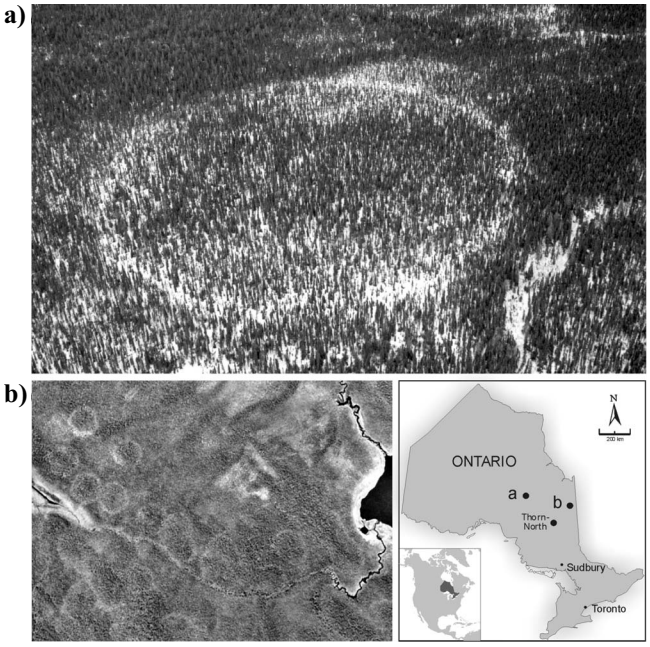

Figure 2. Examples and locations of several forest rings in Ontario. (a) An oblique photograph, taken in winter, of a roughly 300-m-wide ring located south of Hearst, Ontario (N 49° 16′ 05″, W 83° 45′ 01″). (b) A vertical aerial photograph of a cluster of 100-m-wide rings located northeast of Cochrane, Ontario (N 49° 29′ 48″, W 80° 05′ 40″). Inset shows the location of the two rings and the Thorn-North ring (N 48° 46′ 32″, W 81° 40′ 06″) shown in Figure 3.

To better understand the cause of SP anomalies, we measured SP and redox potential over a variety of nonelectronically conductive features, including forest rings in northern Ontario. Such features are useful to study because they lack the complicating effects of SP generated by conduction of electrons (e.g., Sato and Mooney, 1960; Bølviken and Logn, 1975; Thornber, 1975; Govett, 1976) in metallic or semimetallically bonded materials such as sulfide orebodies. This paper presents data from the Thorn-North forest ring and discusses the cause of the SP anomalies.

STUDY AREA

Location

The Thorn-North forest ring is 60 km northwest of Timmins, Ontario (Figure 2). The region is located in the boreal-shield climate zone, characterized by abundant precipitation and hot summers and cold winters of about equal duration.

Forest rings are peculiar circular impressions in boreal forests of northern Canada (Veillette and Giroux, 1999; Giroux et al., 2001) which are commonly hundreds of meters in diameter and centered on accumulations of chemically reduced substances in groundwater, overburden, or rock (Hamilton and Cranston, 2000). The circular outlines (Figure 2a and b) are visible on aerial photographs because of a change in vegetation at the rims of the rings. Their shape and distribution are static, as evidenced by a slight topographic depression in the mineral soil beneath the peaty organic cover (Veillette and Giroux, 1999).

More than 1500 forest rings have been identified in northern Ontario (Hamilton et al., 2004a). Of the 12 rings surveyed so far on the ground, the Thorn-North ring has been studied in the greatest detail because it is the most road-accessible. It is centered on an accumulation of hydrogen sulfide in groundwater, $H_2S_{(aq)}$. Most other forest rings investigated to date occur over shallow accumulations of methane gas, $CH_{4(g)}$ (Hamilton et al., 2004a).

Geology of the study area

The Thorn-North ring (Figure 3) is approximately 580 m in diameter and is situated in a heavily forested area of glacial sediments that are approximately 30 m thick. It occurs on the western margin of a large, 30-km-long, south-southeast-trending esker. In this regard, it is different from most other rings, which typically occur in areas of uniform surficial sediments such as clay or till plain. Fifty-four boreholes (Figure 3) of approximately 8 m depth were drilled in overburden on transects across the ring, and monitoring wells were installed.

Overburden at the depth of the well screens (~7 m) changes abruptly near the center of the ring from glaciolacustrine clay and clay till in the west to esker sands in the east (Figure 4). The esker is draped by a 1–2-m-thick oxidized clay unit to the eastern extent of the sampled line. This is overlain by thin sand beneath discontinuous peat with a typical combined thickness of less than 1 m. An ephemeral perched water table occurs above the clay in the east.

In an area to the southwest affecting the six wells on the southwest axis and four wells on the extremity of the west axis, this deeper clay is overlain by lacustrine sand, 3–6 m in thickness. Peat cover above the clays west of the esker boundary is typically 1 m and locally as much as 2 m thick. Generally, thin humus, but no peat, occurs above the lacustrine sand. Water levels in the monitoring wells indicate

downward hydraulic gradients from the peat into the clay, from the clay into the underlying sand, and from the sand into bedrock across the entire site (Figure 4).

Bedrock was examined by boreholes at three locations on the east-west transect; one outside and two inside the ring (Figure 3). The eastern hole (TN-01) inside the ring encountered a quartz-feldspar porphyry at 30.7 m depth with minor (<2 vol%) disseminated sulfide minerals, predominantly pyrite. The western hole (TN-47) encountered intensely sheared quartz-feldspar porphyry at 36.1 m depth. A third borehole (TN-02), approximately 75 m west of the ring, intersected gabbroic rocks with very minor pyrite at 27.4 m depth.

DATA ACQUISITION

Drilling, well installation, and soil sampling

Monitoring wells were installed using a track-mounted Central Mine Equipment Company drilling rig and 0.2-m-diameter (8-inch) hollow-stem augers. Small 32-mm-diameter ($1\frac{1}{4}$-inch) plastic monitoring wells were installed in each borehole following the methods reported in Hamilton et al. (2004b). In each well, a single screened sampling interval was installed within a graded silica filter pack at a depth of 6.4–7.6 m (21–25 ft) depth and sealed above with bentonite. The depth to static water level in the wells varies from 1–2 m in the west to 3–4 m in the eastern wells (Figure 4). During drilling, soil was sampled at several intervals using a split spoon and sealed in air-tight plastic bags prior to ORP and pH analysis.

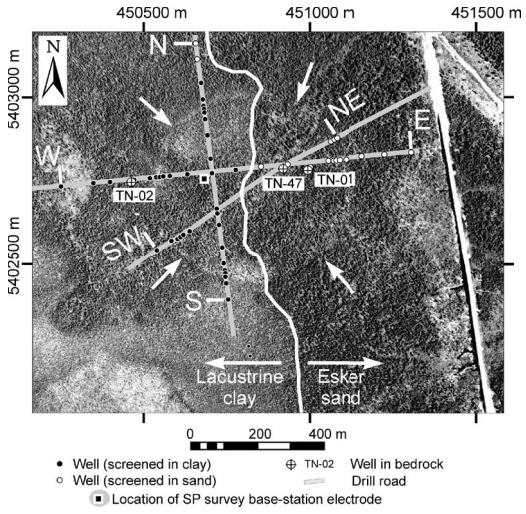

Figure 3. Locations of monitoring wells at the Thorn-North forest ring. White arrows mark the edges of the ring. N-S, E-W, and SW-NE delineate the three sampling transects shown in Figures 4–7. The thick white line shows the western boundary of esker sands as defined by drilling and aerial photograph interpretation. Position of wells relative to each other is accurate to within a few centimeters. Georeferencing of aerial photograph is accurate to ±10 m. Grid units are northings on the vertical axis and eastings on the horizontal axis, and the projection is NAD 1983, UTM Zone 17N (Ontario Ministry of Natural Resources aerial photograph number 91-4826-64-86).

ORP of soils and groundwater

ORP of groundwater was measured in September 2000 using probes (Corning model 476513) with internal silver-silver chloride (Ag-AgCl) reference cells and a pH/mV meter. Prior to ORP measurement, the water level in each well was pumped down, the headspace was purged with $N_{2(g)}$, and vapor locks were installed to prevent oxidation of the slowly recovering waters. The ORP measurements were taken after 4 days of water-level recovery. On a second occasion, 3 weeks later, measurements were made on the standing well water with no preparation of the wells.

Before the start of each traverse, ORP probes were depolarized for 1 hour in water from one of the wells to be tested. Throughout this period, ORP values dropped steadily by approximately 200 mV as the probes lost the oxidizing polarity that they acquire during probe storage. The measurement at each well started with the transfer of water from the screened portion of the well using a peristaltic pump into a flow cell containing two ORP probes and a temperature probe. The values were recorded at 3 minutes after probe immersion. On

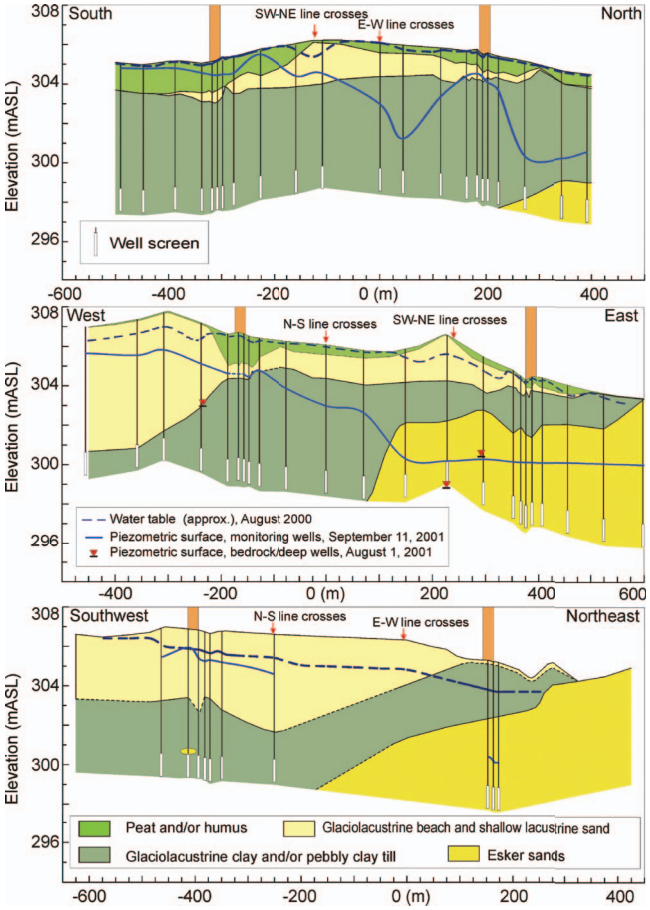

Figure 4. Geologic cross sections at the Thorn-North ring, showing the glacial sedimentary stratigraphy and the position of shallow wells on the transects shown in Figure 3. Vertical orange bars delineate the whitish rim of the ring visible on the aerial photograph in Figure 3. The piezometric surface in bedrock is shown on the east-west transect at the locations of the three deep wells (not shown). Water table depth was observed in auger holes during the soil sampling program. Elevation is shown in meters above sea level (mASL).

each traverse, ORP was measured at the first well and then successively and continuously at each well along that line until all wells had been tested.

The ORP of soil slurries was determined during the drilling program. Samples were collected by split spoon; within an hour of collection, the samples mixed into a 1:1 (by volume) slurry with distilled water and analyzed. ORP values were recorded after 5 minutes of probe immersion. Polarization of the probe during overnight storage in air was reduced by repeating the measurements on the first sample at the beginning of each day. The first set of readings invariably showed higher ORP than the second, and the latter set was recorded as the ORP for that site. The method resulted in good reproducibility from 25 duplicate pairs with a coefficient of determination (R^2 value) of 0.883 for the regression line (Hamilton et al., 2004b).

ORP probes contain platinum electrodes. It is well known that platinum electrodes do not necessarily provide quantitatively reliable redox data for geologic materials (e.g., Lu and Macnae, 1998), partly because of the memory effect that platinum electrodes acquire during storage (Hamilton et al., 2004b). This contributes to the excessively long times (i.e., weeks; Solimin, 1965) that platinum-based probes can take to equilibrate with geologic materials.

In our study, the redox contrast between the target and background areas is important, and full equilibration of the platinum electrodes was neither attempted nor achieved. The protocols just described measure redox with good reproducibility; but because they are not quantitative, the values obtained cannot be converted directly to electrochemical potential or E_h.

Noble metal-based electrodes can provide reliable results when measuring metallic redox couples such as Fe^{2+}/Fe^{3+} but are not ideal for measuring systems in which oxygen ($O_{2(g)}$) contributes significantly to mixed potentials such as water-unsaturated (vadose zone) environments (Bartlett and James, 1995). However, noble-metal-based probes are currently the only instruments available for measuring mixed potentials in the field, and in this study, the relative redox responses they provided were verified by additional redox-indicating parameters, which are described below.

Spontaneous potential

Conventional SP measures differences in electrical potential between two nonpolarizable electrodes, one stationary and another mobile. Our measurements involved using two mobile electrodes, which were lowered into the screened portion of plastic monitoring wells with a uniform depth of approximately 7 m from ground surface (Figure 1). A high-impedance voltmeter was then used to measure voltage between each mobile electrode and a nonpolarizing base-station electrode on the surface near the center of the site (Figure 3).

One of the downhole electrodes was a small nonpolarizing Cu-$CuSO_4$ half-cell electrode similar to that used at the base station. The second consisted of a 20-cm platinum wire wrapped around a plastic core. Using these electrodes together (Figure 1) allows simultaneous determination of electrical field, total field (i.e., the sum of the electrical and redox potentials), and ORP (Timm and Moller, 2001).

In each borehole, measurements were made first with the Cu-$CuSO_4$ electrode and then by the platinum electrode after 1 minute of probe immersion. These are referred to as the SP and PtSP measurements, respectively. Measurements were made on the first well of each traverse and then in each shallow well on that traverse without interruption. All measurements were referenced against a single Cu-$CuSO_4$ base-station electrode located near the 0-m point where the north-south and east-west lines cross (Figure 3). It was placed on freshly exposed, water-saturated peat in a shallow pit and covered to prevent solar warming.

Nonpolarizing electrodes measure voltage across a liquid junction, which causes difficulties when the mobile electrode encounters soils with significantly different moisture content than occurs at the base-station electrode. Osmotic and capillary potentials across the usually ceramic membrane increase with decreasing moisture of the soils and can exceed 60 mV over very short distances (Hamilton et al., 2004b). We encountered this problem in several surface SP surveys over other forest rings, where moisture-related responses exceeded 30 mV. The downhole SP survey at Thorn-North was an attempt to avoid the moisture problem altogether by measuring fully saturated media at both the mobile and base-station electrodes. This eliminated moisture-content differences between these and also between the mobile stations.

The overall SP anomaly obtained (discussed later) was approximately 15 mV, which demonstrates (1) the high degree of sensitivity of the downhole measurements and (2) that moisture-related noise in a surface SP survey would almost certainly have overwhelmed the SP response.

Sulfur species in groundwater

The hydrogen sulfide ($H_2S_{(aq)}$) in groundwater was measured using a field colorimetry kit (Hach model 2238-01), which can determine total sulfide ranging from 0.01 to 11.25 ppm with a precision of 0.01 ppm. The low turbidity of the samples suggests the sulfide species are all dissolved (i.e., H_2S, HS^-, or S^{2-}). The $SO_4^{2-}{}_{(aq)}$ concentrations were determined in the laboratory using an ion chromatograph (Dionex DX300) with a detection limit of 0.01 ppm. The samples were analyzed for SO_4^{2-} up to several months after collection, so the concentrations measured also included a component of SO_4^{2-}, resulting from oxidation of the dissolved sulfide that was present in the water at the time of collection.

Gases in well headspace

The concentrations of $O_{2(g)}$ and $CH_{4(g)}$ were measured in the headspace of wells using an Eagle® portable multigas meter after water levels in the wells had been pumped down and allowed to recover for several days. The data acquisition involved removing the well cap, inserting a tube 50–100 cm into the headspace of the well, and, as the pump inside the instrument withdrew the gases, recording the minima and maxima of the concentrations of $O_{2(g)}$ and $CH_{4(g)}$, respectively. The $O_{2(g)}$ measurement, by the electrochemical cell method, has an accuracy of $\pm 5\%$ and a resolution of 0.1% of the measured value. The concentration of $CH_{4(g)}$ was determined from the total combustible gases by platinum catalysis, calibrated to CH_4, and has an overall accuracy of $\pm 5\%$ of the value and a resolution of 5 ppm.

The consumption of $O_{2(g)}$ in the headspace during water-level recovery provides an approximation of the availability of reducing agents in the recovering waters. Methane is produced biologically in reduced environments; therefore, its presence or absence in the well headspace provides a qualitative indication of the redox conditions in the aquifer.

RESULTS

Redox parameters

All of the redox-indicating parameters show a negative redox response from the outside to the inside of the ring, manifested at its edges. This is particularly evident to the north, west, and east. The ORP measurements on groundwater (Figure 5a) show a sharp decline from the outside to the inside of the ring on the east, west, and southwest edges. There are too few wells on the northeast boundary to assess the response, and reliable groundwater ORP data do not exist for the north-south line.

Soil-slurry ORP data from the 2-m depth show a decrease at the boundaries of the ring from outside to inside (Figure 5b). Near the eastern boundary, the change is gradual, reflecting the presence of the thin oxidized clay unit that drapes the esker (Figure 4). As mentioned, unsaturated sand underlies this clay unit, and some or all of these samples may have been from the vadose zone. The north-south transect shows a sharp change at the ring boundaries, which takes the form of lows with minor flanking highs. On the north-south line (Figure 5), the scale was expanded to highlight the redox response at the ring edges. The magnitude of the redox contrast outside and inside the ring is lower on this line because the soil medium is consistently reduced clay, except in the northernmost two samples, which are somewhat oxidized.

In groundwater from the two bedrock wells inside the ring (Figure 3), high H_2S concentrations of 11.0 (well TN-47) and 2.25 (well TN-01) ppm were recorded. Relatively low SO_4^{2-} concentrations of 7.3 and 3.8 ppm, respectively, were recorded for these same waters. Mass-balance calculations suggest that most or all of the SO_4^{2-} in the bedrock groundwaters may have resulted from oxidation of their H_2S during the collection and transport of the samples. The data indicate that the groundwaters in bedrock are highly reduced.

The available H_2S data for groundwater from shallow wells (Figure 6a) show higher concentrations inside the ring and a sharp drop at the boundaries. The SO_4^{2-} in groundwater from the overburden wells shows elevated concentrations across the ring, particularly where samples were collected from clay on the north-south transect and the west axis (Figure 6a). The SO_4^{2-} also shows very high spikes in concentration at the ring edges on the east, southwest, and northeast axes, precisely where H_2S concentrations drop. This indicates that oxidation of $H_2S_{(aq)}$ to $SO_4^{2-}{}_{(aq)}$ occurs in shallow groundwater across the ring but is particularly pronounced at the boundaries. It also shows the boundaries represent an abrupt transition from a reduced regime inside the ring, where H_2S and SO_4^{2-} coexist, to an oxidized regime outside, where SO_4^{2-} is the dominant sulfur species.

The $O_{2(g)}$ content (Figure 6b) in the headspace of wells is lower inside the ring relative to outside, particularly for wells with screens finished in clay on the north-south transect and the west and southwest axes. A substantial depletion in $O_{2(g)}$ occurs at the ring edges, which is again more pronounced in wells finished in clay. The $CH_{4(g)}$ in the well headspace is generally low inside and outside the ring but shows spikes in concentration at the ring boundaries (Figure 6b), which suggests increased anaerobic microbial activity in these areas.

The redox measurement (Figure 7) determined during the downhole SP survey is a calculated parameter obtained by subtracting the electrical potential measurement (SP) from the total field measurement (PtSP) to yield the chemical (redox) component of voltage (Figure 1). These data (Figure 7) show generally lower values inside

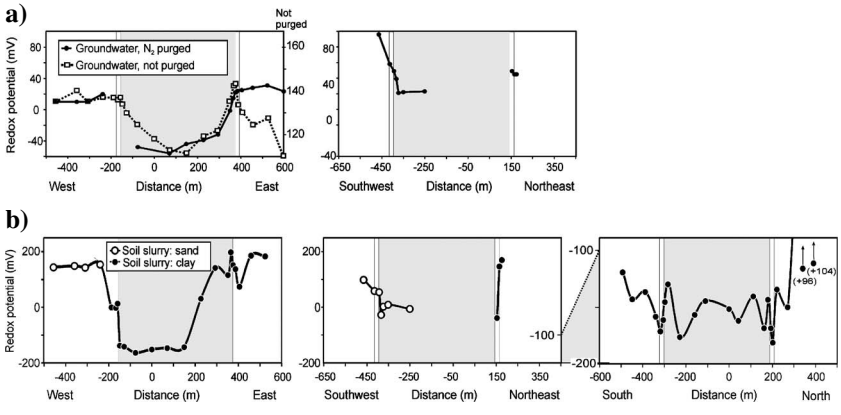

Figure 5. Redox potential on the three transects shown in Figure 3. (a) Redox potential (ORP) of groundwater, September 2000. The scale on the left of each figure shows ORP measured on fresh groundwater extracted from shallow wells following the purging procedure described in the text. The scale on the right of the west-east transect shows ORP measured on standing well water. (b) Redox potential measured within one hour of sampling on soil slurries collected during the March 2000 drilling program. Gray boxes show the extent of the ring and white margins show the position of the whitish rim that delineates the ring edge.

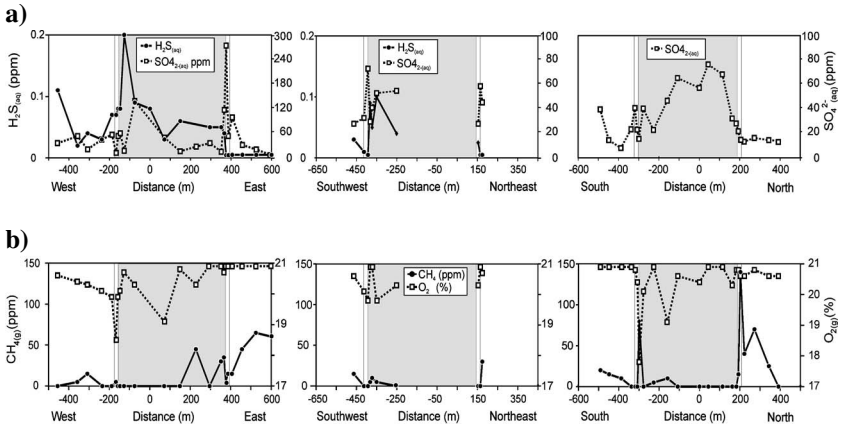

Figure 6. Redox-sensitive parameters on the three transects shown in Figure 3. (a) Dissolved sulfate and sulfide measured in groundwater extracted from shallow monitoring wells in September 2000 and July 2002, respectively. The H_2S concentrations are shown on the left axis, and sulfate concentrations are on the right. Field conditions (a forest fire) prevented the collection of H_2S data on the north-south transect. (b) Gas measurements made in the headspace of wells in July 2000, following the pumping down of water levels and several days of recovery. The CH_4 concentrations are shown on the left, and oxygen concentrations are on the right of each figure. The significance of the gray and white outlines is as in Figure 5.

the ring and negative excursions on the inside boundaries, which is consistent with the other redox-related parameters. This is particularly evident to the north, west, and east. The response is unclear to the south because the electrode became negatively polarized by extremely reducing conditions in the third most-southerly well; this polarization affected the readings in the remaining two wells.

The reducing conditions in this well are thought to have resulted from the accidental use, during well construction, of bentonite pellets with a biodegradable coating. This appears to have created more reduced conditions in the well water here than in the other wells that were constructed with untreated bentonite chips.

SP anomalies

The SP data on the north-south and east-west traverses show positive downhole excursions in electrical potential over the ring (Figure 7) relative to adjacent soils surrounding it when both are referenced to the central base-station electrode on surface (Figure 3). The only exception is a single value in a well located at +150 m on the east-west transect (Figure 7). This well occurs at the boundary between clays to the west and sand to the east at a point where the piezometric data indicate groundwater discharges from the clay eastward and then downward into the sand (Figure 4). Its more negative response may be caused by streaming potentials related to this phenomenon.

Considering the heterogeneous composition of soil and overburden in the area, the similar pattern of SP variation across the east-west and north-south transects is remarkable.

DISCUSSION

General mechanism of ring formation

The proposed mechanism for ring formation (Hamilton, 2005) is shown in Figure 8. The rings are all centered on some source of negative charge such as methane or dissolved sulfide, which maintains iron, transitional metals, and/or sulfur species in a reduced state in overburden within the ring. The oxidation of these species at the edge of the reduced area produces acid, which dissolves carbonate in soils and results in a depression. In the boreal forest, swampy conditions occur in the resulting circular depression (Giroux et al., 2001). In the subsurface, the result across the entire ring includes decreased redox, depleted oxygen, and elevated concentrations of reduced species. At the ring edge, the products include very strong redox gradients, decreased pH, depleted carbonate, increased $CO_{2(aq)}$, and increased metals in soil.

The strong redox and concentration gradients induce the outward migration of reduced species toward the more oxidized conditions at the edge of the ring. The mechanism that moves these species is indicated by the excellent circularity of the rings. To produce circles, the overburden must be isotropic with respect to the transport process. Glacial overburden materials saturated with fresh groundwater are likely to have reasonably isotropic electrical conductivity but highly anisotropic permeability. This is especially the case at Thorn-North, where the hydraulic conductivity rises by more than three orders of magnitude from west to east. This precludes advection, diffusion, or gaseous transport as possible ring-formation mechanisms and supports the redox-gradient transport model of Hamilton (1998, 2000).

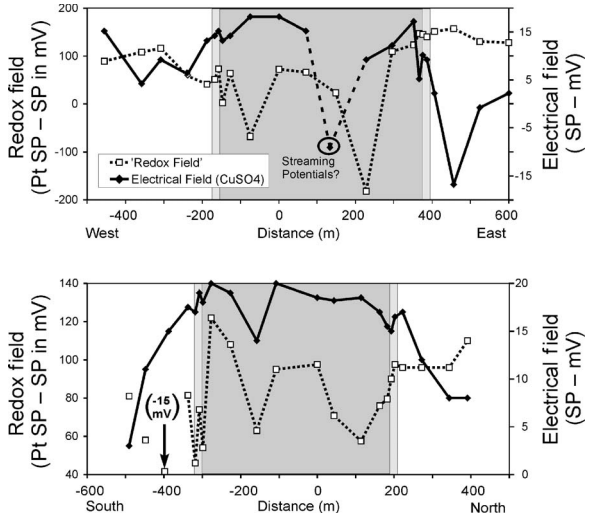

Figure 7. Downhole SP (right axis) and calculated redox (left axis) for the east-west and north-south transects of the Thorn-North ring from a survey carried out in September 2000. The electrical field and redox parameters are related to one another as discussed in the text and shown in Figure 1. All measurements were taken against a single Cu-$CuSO_4$, nonpolarizing, base-station electrode located on surface near the 0-m point, shown on Figure 3. The reading at −400 m on the south line was offscale and is shown on the figure in parentheses. The low reading near +150 m on the east-west line may be caused by streaming potentials, as discussed in the text.

Covariation of SP anomalies and redox parameters

Strongly reducing conditions in bedrock underlying the ring are demonstrated by high concentrations of $H_2S_{(aq)}$ in groundwater and very low concentrations of $SO_4^{2-}{}_{(aq)}$ (Figure 6a). In the shallow overburden inside the ring, $H_2S_{(aq)}$ concentrations are lower but still measurable, and $SO_4^{2-}{}_{(aq)}$ concentrations are much higher, indicating a moderately reduced regime. In the shallow overburden, an abrupt transition to an oxidized regime occurs at the ring boundaries, as

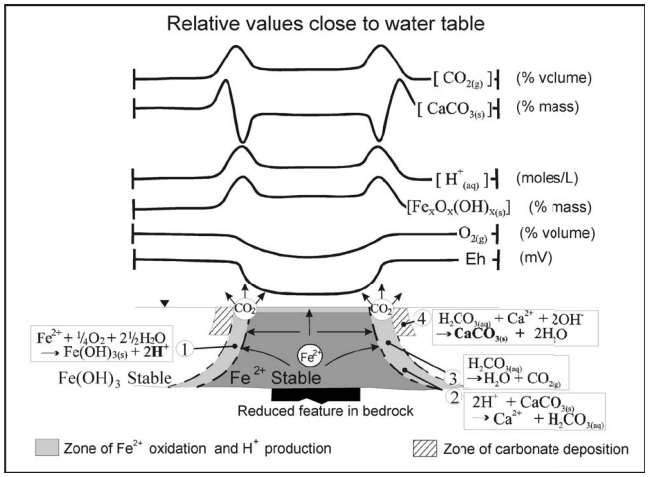

Figure 8. Theory of ring formation. At the redox boundary at the ring edge, oxidation of transitional metals and/or sulfur species produces H^+ (1), which dissolves carbonate in mineral soil (2), producing $CO_{2(aq)}$ (3). Carbonate depletion causes a topographic depression around the rim of the ring, which results in wetter conditions, diminished tree growth, and a lighter-colored rim around the ring that is visible from the air. Reprecipitation of carbonate (4) outside the rim may also contribute to the visibility of the ring (modified after Hamilton, 2000).

demonstrated by a sharp reduction in H_2S concentration and by other redox-indicating parameters, especially groundwater ORP.

An increase in molar ratios of SO_4^{2-}/H_2S in groundwater inside the ring from <0.23 in bedrock to an average of >800 in shallow overburden, suggests H_2S is fluxing upward in the ring and oxidizing in the shallow subsurface where $O_{2(aq)}$ is more abundant. This is supported by the generally lower $O_{2(g)}$ in the headspace of recovering wells within the ring. The very high spikes in SO_4^{2-} at the ring edges, which are coincident with a drop in H_2S and $O_{2(g)}$ concentrations, suggest the remaining H_2S in shallow overburden is fluxing outward to the ring edges, where it encounters an abruptly higher redox regime and oxidizes to SO_4^{2-}.

The observed variation in redox-sensitive parameters demonstrates that chemically reduced conditions occur inside the ring and strong redox gradients occur at the edges, although a detailed discussion of the redox chemistry is beyond the scope of this article. At several of the ring edges, the oxidation potential within the ring increases outward by several hundred millivolts over the 10 m separating one well from the next. The redox boundary appears to be nearly vertical and occurs to a depth of at least 7 m. Therefore, the forest ring is a visual manifestation of a large, circular reduced chimney (Hamilton et al., 2004b, 2004c) in overburden, although the origin of the H_2S accumulation in rock upon which it is sourced is not currently known.

The spatial correlations between positive SP and the negative redox responses over the ring in the absence of any conductor of electrons suggest that the causes of SP anomalies may be related to redox changes.

Previously proposed interpretations of SP anomalies

Although no known mineral deposit occurs in association with the Thorn-North forest ring, it is similar to some mineral deposits because it represents a negative redox anomaly in the subsurface and has an associated SP anomaly. However, it differs from most mineral deposits because the SP anomaly is positive, relative to soils adjacent to the ring. Various models have been proposed to explain SP anomalies over mineral deposits. They include (1) dipole-conductor models, (2) a measurement-artifact model that argues against the presence of an electrical field over mineralization, and (3) a permanent ferroelectric polarity model.

Various dipole-conductor models (model 1) have been proposed to explain SP anomalies over steeply dipping electronically conductive mineral deposits (e.g., Schlumberger and Schlumberger, 1922; Sato and Mooney, 1960; Bølviken and Logn, 1975; Thornber, 1975; Govett, 1976; Hamilton, 1998). They argue that differences in oxidation potential in the groundwater environment between the top and bottom of the conductor cause it to polarize with a negative (cathodic) pole in the shallow oxidized environment and a positive (anodic) pole at depth. This causes a negative SP response above the conductor.

The dipole models cannot account for the large SP responses reported over disseminated sulfides and oxide caps (Burr, 1982; Corry, 1985; Goldie, 2002) or over other reduced and nonelectronically conductive features such as oil reservoirs (Campbell, 1960; Pirson, 1981). They also require large, grain-interconnected, electronically conductive (i.e., with metallic or semimetallic bonding) bodies and are therefore not applicable to Thorn-North, where no continuous electronic conductors are present.

Model 2 proposes that SP anomalies over mineral deposits are a measurement artifact resulting from different oxidation potentials in soils encountered by the two electrodes (Corry, 1985). It is argued that the lower oxidation potential of soils over the mineral deposit relative to background areas would induce an electrical potential between the stationary and mobile electrodes that would not occur without the wire connecting them. Therefore, the SP apparatus responds to a difference in redox potential and no electrical field necessarily exists in association with the ore deposit. This model is used by Nyquist and Corry (2002) to explain the SP anomalies observed over organic waste plumes in shallow aquifers.

We consider the development of SP voltages in response to nonpolarizing electrodes encountering soils with different oxidation potentials to be inconsistent with the SP data obtained by later workers. For example, Timm and Moller (2001) demonstrate theoretically and experimentally that SP responses measured using nonpolarizing electrodes are not affected by different oxidation potential of soils and respond only to differences in electrical potential. This is confirmed by Hamilton et al. (2004c). Furthermore, Corwin and Hoover (1979) observe that when using nonpolarizing electrodes, chemical potentials in soils produce biases of only several tens of millivolts caused by contamination of the electrolyte. This contrasts with biases when using bare metallic electrodes, which can reach hundreds of millivolts and result from the chemical potential of both the metal electrode and the soil it contacts (Schlumberger, 1920).

Model 3 suggests that a permanent ferroelectric polarity exists in some ore deposits (Corry, 1994) and can result in a measurable SP on surface. Ferroelectricity is a property of certain solids whereby the electrical dipoles of constituent molecules have a preferred alignment that imparts a macroscopic electrical polarity to the whole solid. A permanent ferroelectric polarity in an ore deposit would require the existence of an initial electrical field and the retention of that property by minerals as they cooled to below their Curie temperature. The electrical fields associated with ferroelectric solids are static. Therefore, as the sole mechanism responsible for SP anomalies, this model fails to explain mass transport and geochemical anomalies commonly associated with SP anomalies. Corry (1994) field tests this model and finds no evidence that ferroelectric ore minerals produce a measurable SP effect on surface.

Origin of SP anomalies over the forest ring

The forest ring studied does not contain significant quantities of metallic phases (i.e., that have metallic or semimetallic bonding) and, as such, does not exhibit electronic conduction. Notwithstanding, a distinct positive SP response occurs over the ring relative to adjacent soils when both are measured against the same base-station electrode.

Very strong, outward-increasing redox gradients occur around the perimeter of the Thorn-North forest ring, which are coincident with inward-increasing concentrations of dissolved sulfide. Any polarizable substance within this gradient, such as a sulfide grain, will develop a polarity with its negative electrical pole in the positive redox direction, where electron acceptors are more prevalent. However, no metallic phases are known to occur in the saturated overburden where the redox gradients were measured.

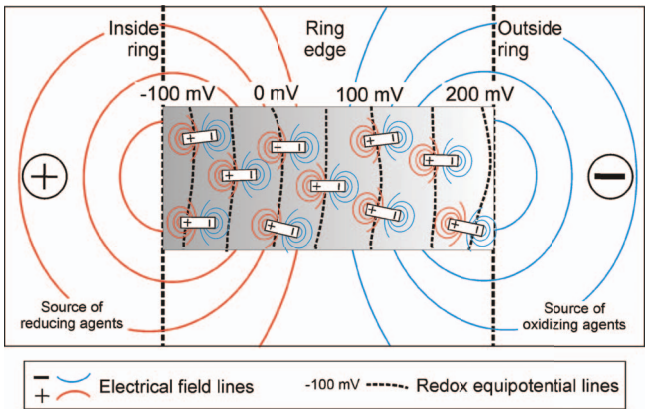

Figure 9. Diagram showing the development of redox-induced spontaneous polarization at the ring edge. (1) A strong, preexisting redox gradient polarizes redox-active ions and colloids with their negative poles pointing toward oxidizing agents (electron acceptors) in the positive redox direction. (2) Mutual alignment of the constituent electrical fields of all the polarized ions will produce (3) a resultant field that is also negative in the direction of positive redox charge. Redox-active species are those that are capable, or nearly capable, of spontaneous redox reaction in the electrochemical environment they occupy. In contrast, redox-inert species, such as Na^+ and Cl^-, cannot be oxidized or reduced within the natural limits of water stability. Values were arbitrarily assigned to the redox equipotentials to illustrate a redox gradient that increases to the right, toward the outside of the ring.

The above-neutral pH of groundwater indicates the predominant sulfide species is $HS^-_{(aq)}$, which is a polar molecule. In a strong redox gradient, the lowest energy rest state of the HS^- molecule should be with its negative pole pointing in the positive redox direction, i.e., toward neighboring species that have the strongest affinity for electrons. A general negative-outward polarity to HS^- and other redox-active, polar species such as water will result in a macroscopic electrical polarity to the redox gradient as a whole and electrical (SP) anomalies that are negative at the oxidizing end of the redox gradient (Figure 9). The redox gradients around the perimeter of the ring are near-horizontal, so this should impart a net positive SP response in surface soils inside the ring relative to outside, as has been observed.

The strong concentration gradient of sulfide species around the perimeter will induce an outward diffusive flux of HS^- that will perpetuate the redox gradient despite ongoing oxidation reactions that would otherwise diminish it, along with any associated electrical field.

CONCLUSION

When measured using a single, centrally located base station, the Thorn-North forest ring exhibits a positive SP response in shallow overburden across the ring, which correlates with a negative redox anomaly in the same materials, caused by an accumulation of HS^-. We propose that the positive electrical response is caused by an electrical polarity to redox-active ions that constitute the redox gradient around the perimeter of the ring. This redox-induced spontaneous polarization is argued to result from preferred orientation of redox-active ions and polar molecules within the redox gradient such that the negative ends of the dipoles point in the positive (oxidizing) redox direction, toward the neighboring species with the stronger affinity for electrons. Maintaining reducing conditions inside the forest ring and strong redox gradients at the edge, in the overall oxidized surface environment, requires a steady state outward flux of reduced molecules or ions. This is facilitated by the outward diffusion of HS^- in the concentration gradient at the perimeter of the ring. It is also proposed that because the resulting macroscopic electrical field occurs in an aqueous medium, some of its constituent species are free to move as a result of the induced electrical field.

ACKNOWLEDGMENTS

The authors would like to thank Diatreme Explorations Inc. for providing drill-road access to the Thorn-North site and sharing technical information. Devin Cranston and Boris Iotzov provided excellent assistance in the field and laboratory. We would also like to thank an anonymous commenter from the audience at a presentation to the Edmonton Chapter of the Geological Association of Canada that Hamilton delivered in May 2003. His comments on electrical polarization of solids, and Corry's (1994) paper, contributed significantly to our thinking on this subject.

REFERENCES

Bartlett, J. B., and R. J. James, 1995, System for categorizing soil redox status by chemical field testing: Geoderma, **68**, 211–218.
Bølviken, B., and O. Logn, 1975, An electrochemical model for element distribution around sulfide bodies, *in* I. Elliot and K. Fletcher, eds., Geochemical exploration 1974: Developments in Economic Geology 1, 631–648.
Burr, S. V., 1982, A guide to prospecting by the self-potential method: Ontario Geological Survey Miscellaneous Paper 99, 1–15.
Campbell, O. E., 1960, Why sedimentary structures show high self potentials: World Oil, **150**, 97–98.
Corry, C. E., 1985, Spontaneous polarization associated with porphyry sulfide mineralization: Geophysics, **50**, 1020–1034.
———, 1994, Investigation of ferroelectric effects in two sulfide deposits: Journal of Applied Geophysics, **32**, 55–72.
Corwin, R. F., and D. B. Hoover, 1979, The self-potential method in geothermal exploration: Geophysics, **44**, 226–245.
Giroux, J. F., Y. Bergeron, and J. J. Veillette, 2001, Dynamics and morphology of giant circular patterns of low tree density in black spruce stands in northern Quebec: Canadian Journal of Botany, **79**, 420–428.
Goldie, M., 2002, Self-potentials associated with the Yanacocha high-sulfidation gold deposit in Peru: Geophysics, **67**, 684–689.
Govett, G. J. S., 1976, Detection of deeply buried and blind sulfide deposits by measurement of H^+ and conductivity of closely spaced surface soil samples: Journal of Geochemical Exploration, **6**, 359–382.
Hamilton, S. M., 1998, Electrochemical mass-transport in overburden: A new model to account for the formation of selective leach geochemical anomalies in glacial terrain: Journal of Geochemical Exploration, **63**, 155–172.
———, 2000, Spontaneous potentials and electrochemical cells, *in* G. J. S. Govett and M. Hale, eds., Handbook of exploration geochemistry, vol. 7: Elsevier Scientific Publ. Co., Inc., 81–119.
———, 2005, The development of giant ring structures over buried sources of negative charge: Ontario Prospectors Association and Ontario Geoscience Symposium, accessed December 5, 2007; www.mndm.gov.on.ca/mndm/mines/ogs/posters/OEGS_2005/OEGS-Hamilton.pdf.
Hamilton, S. M., A. K. Burt, K. H. Hattori, and J. Shirota, 2004a, The distribution and source of forest ring-related methane in northeastern Ontario, *in* Summary of field work and other activities: Ontario Geological Survey Open File Report 6145, 21-1–21-26.
Hamilton, S. M., E. M. Cameron, M. B. McClenaghan, and G. E. M. Hall, 2004b, Redox, pH and SP variation over mineralization in thick glacial overburden — Part I: Methodologies and field investigation at Marsh Zone gold property: Geochemistry: Exploration, Environment, Analysis, **4**, 33–44.
———, 2004c, Redox, pH and SP variation over mineralization in thick glacial overburden — Part II: Field investigations at the Cross Lake VMS property: Geochemistry: Exploration, Environment, Analysis, **4**, 45–58.
Hamilton, S. M., and D. R. Cranston, 2000, Thick overburden geochemistry — methods and case studies, *in* Summary of field work and other activities 2000, Ontario Geological Survey Open File Report 6032, 47-1–47-18.
Lu, K., and J. Macnae, 1998, The international campaign on intercomparison

between electrodes for geoelectrical measurements: Exploration Geophysics, **29**, 484–488.
Nyquist, J. E., and C. E. Corry, 2002, Self-potential: The ugly duckling of environmental geophysics: The Leading Edge, **5**, 446–451.
Pirson, S. J., 1981, Significant advances in magnetoelectrical exploration, *in* B. Gottlieb, ed., Unconventional methods in exploration for petroleum and natural gas, 169–196.
Sato, M., and H. M. Mooney, 1960, The electrochemical mechanism of sulfide self-potentials: Geophysics, **25**, 226–249.
Saunders, D. F., K. R. Burson, and C. K. Thompson, 1999, Model for hydrocarbon microseepage and related near-surface alterations: AAPG Bulletin, **83**, 170–185.
Schlumberger, C., 1920, Essais de prospection électrique du sous-sol: Comptes Rendes, Académie des Sciences, **170**, 519–521.
Schlumberger, C., and M. Schlumberger, 1922, Phénomènes électriques produits par les gisements métalliques: Comptes Rendes, Académie des Sciences, **174**, 477–480.
Solomin, G. A., 1965, Methods of determining Eh and pH in sedimentary rocks (authorized translation from Russian by P. P. Sutton): Consultants Bureau.
Thornber, M. R., 1975, Supergene alteration of sulfides — I: A chemical model based on massive sulfide deposits at Kambalda, Western Australia: Chemical Geology, **15**, 1–14.
Timm, F., and P. Moller, 2001, The relation between electric and redox potential: Evidence from laboratory and field measurements: Journal of Geochemical Exploration, **72**, 115–128.
Tomkins, R., 1990, Direct location technologies: A unified theory: Oil & Gas Journal, **24**, 126–134.
Vagshal, D. S., and S. D. Belyaev, 2001, Self-potential anomalies in Cerro de Pasco and Hualgayoc areas (Peru) revisited: Geophysical Prospecting, **49**, 151–154.
Veillette, J. J., and J. F. Giroux, 1999, The enigmatic rings of the James Bay lowland — A probable geological origin: Geological Survey of Canada Open File Report 3708, 28.